ERDC TN-24-2
January 2024

Preliminary Permafrost Predictions within the Chena River Watershed, Alaska, Using Landscape Characteristics

By Ross E. Alter, Nawa Raj Pradhan, Anna M. Wagner

PURPOSE: This Technical Note presents a method to create permafrost predictions in the Chena River watershed near Fairbanks, Alaska, using landscape characteristics. We produced probabilities for near-surface permafrost in the Chena River watershed using a published algorithm applied in a nearby region. The methodology presented serves as a proof of concept for developing permafrost maps using similar data in other cold regions.

INTRODUCTION: Permafrost is soil that has been frozen for at least two consecutive years. Identifying the probability of permafrost existence and its underlying locations is important for numerically coupled hydrodynamics and thermal dynamics simulations (Pradhan et al. 2013; Pradhan et al. 2019), especially in high-latitude and high-altitude regions. Since characterizing permafrost is an important prerequisite for developing advanced hydrologic models, it is important to have a prediction of permafrost coverage in discontinuous permafrost regions despite sparse observational networks in its most likely locations. This technical note summarizes the method used to predict near-surface permafrost in a watershed in central Alaska—the Chena River watershed (Figures 1 and 2)—and presents preliminary results from the permafrost prediction method.

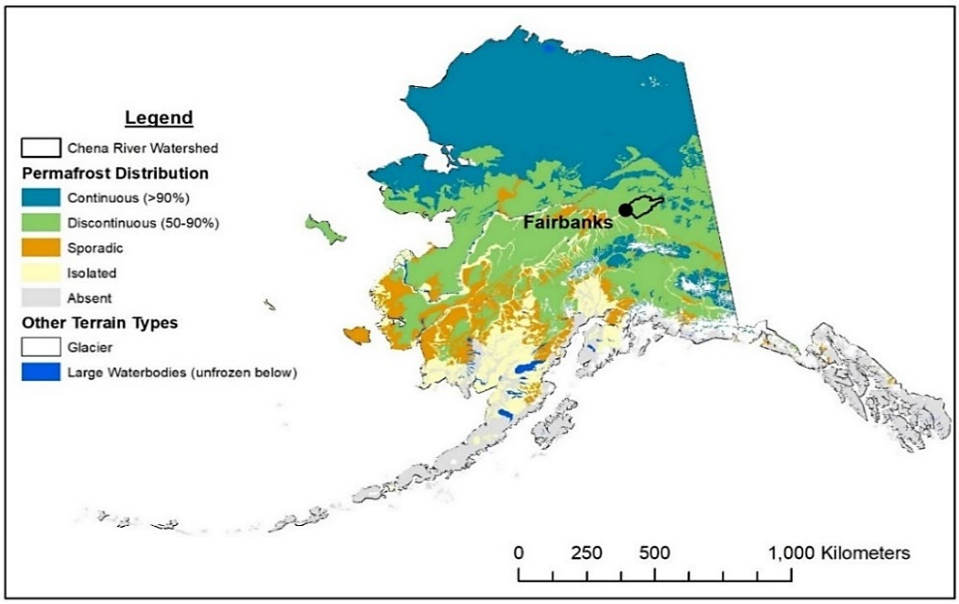

Figure 1. Permafrost map of Alaska, and location of the Chena River watershed. (Image modified from Jorgenson et al. 2008. Public domain.)

US Army Corps of Engineers®

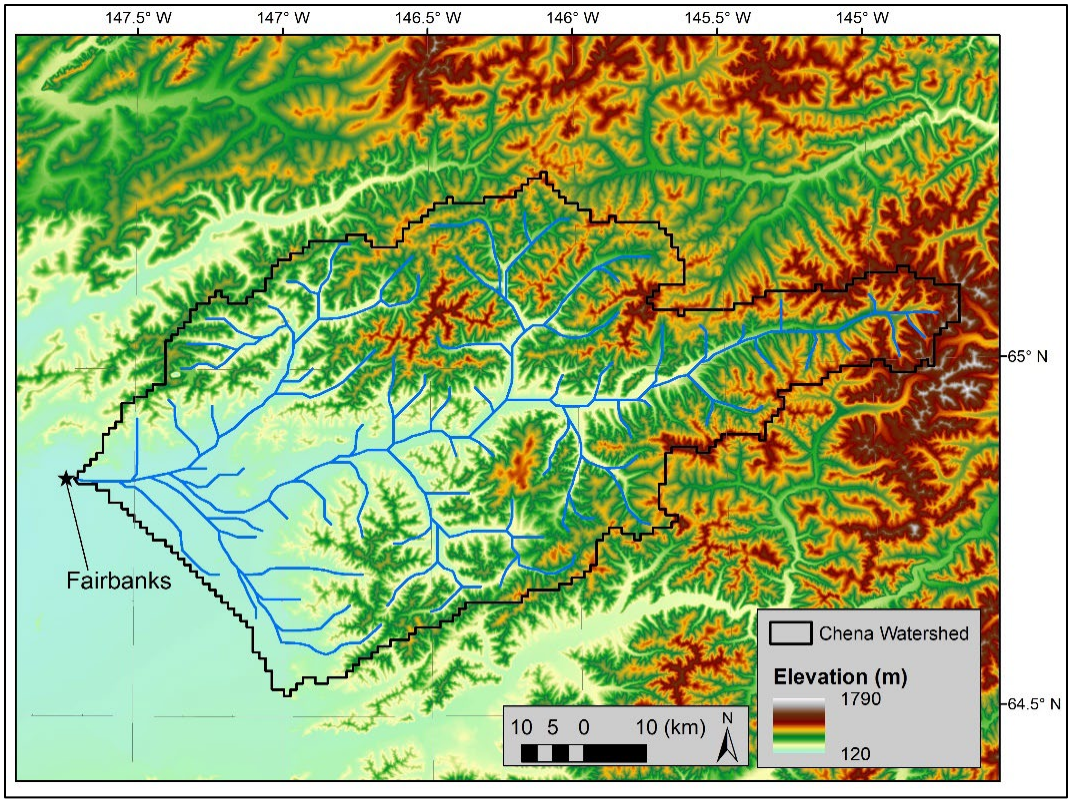

Figure 2. Map of the river network (*blue segments*) and elevation (*multicolor background*) within the Chena River watershed (*black line*) and its surroundings. (Map was created using a digital elevation model with 1 arc-second resolution, USGS 2023.)

METHODS: The permafrost prediction method described in this study is largely based on the methodology of Panda et al. (2010). They used data from remote sensing and field measurements to predict the probability of near-surface permafrost occurrence (within 1.6 m of the surface), Π, in a region in central Alaska:

$$\Pi = \frac{1}{1+ e^{-Z}}, \tag{1}$$

where Z is the sum of the coefficients for elevation, aspect and topography, and land use. The coefficients are obtained via a binary logistic regression model, a form of regression used by Panda et al. (2010) to obtain one of two categorical outputs given a series of categorical or continuous inputs. Using the Panda et al. (2010) methodology, near-surface permafrost is deemed to be present for $\Pi \geq 0.5$ and not present for $\Pi < 0.5$. In our study, we also applied a methodology similar to that employed in recent reports from the Intergovernmental Panel on Climate Change (IPCC), in which textual categories were assigned to numerical likelihoods of a particular outcome (Mastrandrea et al. 2010; Arias et al. 2023). Using this method, three categories were used: "likely" (probability > 0.666666), "unlikely" (probability < 0.333333), and a middle category—"inconclusive" (probabilities between 0.333333 and 0.666666).

Since the Panda et al. (2010) study occurred in central Alaska, the same general region as the Chena River watershed, we extended their methodology to obtain a first-order prediction of near-surface permafrost in our study region. To predict permafrost in the Chena River watershed, we obtained gridded data with 1 km horizontal resolution for land use, aspect, slope, and elevation and categorized the values with coefficients listed in Table 1. For example, a northwest aspect, which largely faces away from the solar path and may therefore be more conducive to permafrost formation, has a positive coefficient (17.95), while a southwest aspect, which largely faces toward the solar path and may therefore be less conducive to permafrost formation, has a negative coefficient (–20.15). In the vegetation class, there was a disconnect between the subclasses used in Panda et al. (2010) and the categories used by the National Land Cover Database (NLCD) (NLCD 2019), which comprised our land use data. For example, though Panda et al. (2010) had an "aspen" subclass, NLCD did not; additionally, there were many more categories in NLCD than in Panda et al. (2010). Therefore, we congealed the NLCD categories into the Panda et al. (2010) subclasses, trying to match their physical characteristics as closely as possible. Because "aspen" is more specific than any of the NLCD categories, we did not include any of the broader NLCD categories in this subclass.

Table 1. Input variable classes and subclasses, descriptions, and coefficients (adapted from Panda et al. 2010). The Description column shows land use categories from the National Land Cover Database (NLCD 2019) that are deemed equivalent to the vegetation subclasses. The NLCD ID numbers are in parentheses. Descriptions for "aspect and topography" and elevation are from Panda et al. (2010).

Class	Subclass	Description (NLCD ID)	Coefficients
Vegetation	Aspen	None	−19.62
	Dense tall spruce	Evergreen forest (42)	1.34
	Scattered short spruce	Dwarf scrub (51), shrub/scrub (52), woody wetlands (90)	21.66
	Deciduous	Deciduous forest (41)	−36.79
	Mixed spruce and deciduous	Mixed forest (43)	0.00
	Wetland meadow	Grassland/herbaceous (71), sedge/herbaceous (72), pasture/hay (81), cultivated crops (82), emergent herbaceous wetlands (95)	−20.15
Aspect and topography	North	337.505°, −22.504°	19.88
	Northeast	22.505°, −67.504°	0.38
	East	67.505°, −112.504°	0.35
	Southeast	112.505°, −157.504°	−0.32
	South	157.505°, −202.504°	−0.02
	Southwest	202.505°, −247.504°	−20.15
	West	247.505°, −292.504°	7.91
	Northwest	292.505°, −337.504°	17.95
	Low-lying flat surfaces	Slope < 8°	0.00
Elevation	Lower	<640 m	0.00
	Higher	≥640 m	1.40

The main land use subclasses in the Chena River watershed are shrub/scrub (52), deciduous forest (41), and evergreen forest (42) (Figure 3*a*). There is also a pocket of grassland/herbaceous (71) in the south-central portion of the region. Along the western edge of the region, there is a mix of developed areas (open space [21] and low intensity [22]) and woody wetlands (90). Overall, the area seems to be characterized by a combination of forest and shorter vegetation.

The aspect subclasses (Figure 3*b*) reflect the varied topography of the region. All subclasses of aspect are represented in the Chena River watershed. More southward-facing aspect values (approximately 180°) are indicated in lighter colors, while more northward-facing aspect values (close to 0° and 360°) are in darker colors. The location of the main river channel within the Chena River network can be seen stretching from west-southwest (WSW) to east-northeast (ENE) along the boundary of light and dark aspects (Figures 2 and 3*c*).

Elevation (Figure 3*c*) generally rises from west to east within the watershed, ranging from 134 m to 1,381 m. Most of the higher elevations are in the eastern portion of the watershed, but there are scattered areas of higher elevation in the central portion of the watershed as well. Similar to the aspect plot, the main channel for the Chena River can be seen extending upstream from WSW to ENE (in *green-blue*).

Like aspect, slope (Figure 3*d*) also reflects the varied topography of the region. Some steeper slopes are evident in the north-central, southern, and eastern portions of the watershed. Note that the red ring around the edge of the domain is spurious (with a similar but weaker effect evident in Figure 3*b*); this will be removed in future efforts.

Land use has a complex arrangement of coefficients throughout the domain (Figure 4*a*). Generally, it seems that positive coefficients are present in the northern and eastern portions of the domain, while negative coefficients are more common in the southern, central, and western portions of the domain. Many of the areas have relatively high coefficients (absolute value >20).

“Aspect and topography” have smaller coefficients overall, with the largest magnitudes of coefficients along the northern and western edges of the domain (Figure 4*b*). There are also scattered areas within the domain itself that have larger absolute magnitudes of values, but most values are close to zero.

Elevation has very small coefficients overall, which is consistent with the definitions in Table 1 (Figure 4*c*). The highest coefficients correspond with the highest elevations along a path extending from north to east to south within the watershed.

The sum of the coefficients is dominated by the land use coefficients (Figure 4*d*). There are some areas where aspect seems to change the sign of the sum (e.g., the southwestern edge), but overall, land use largely controls the sign of the sum of coefficients.

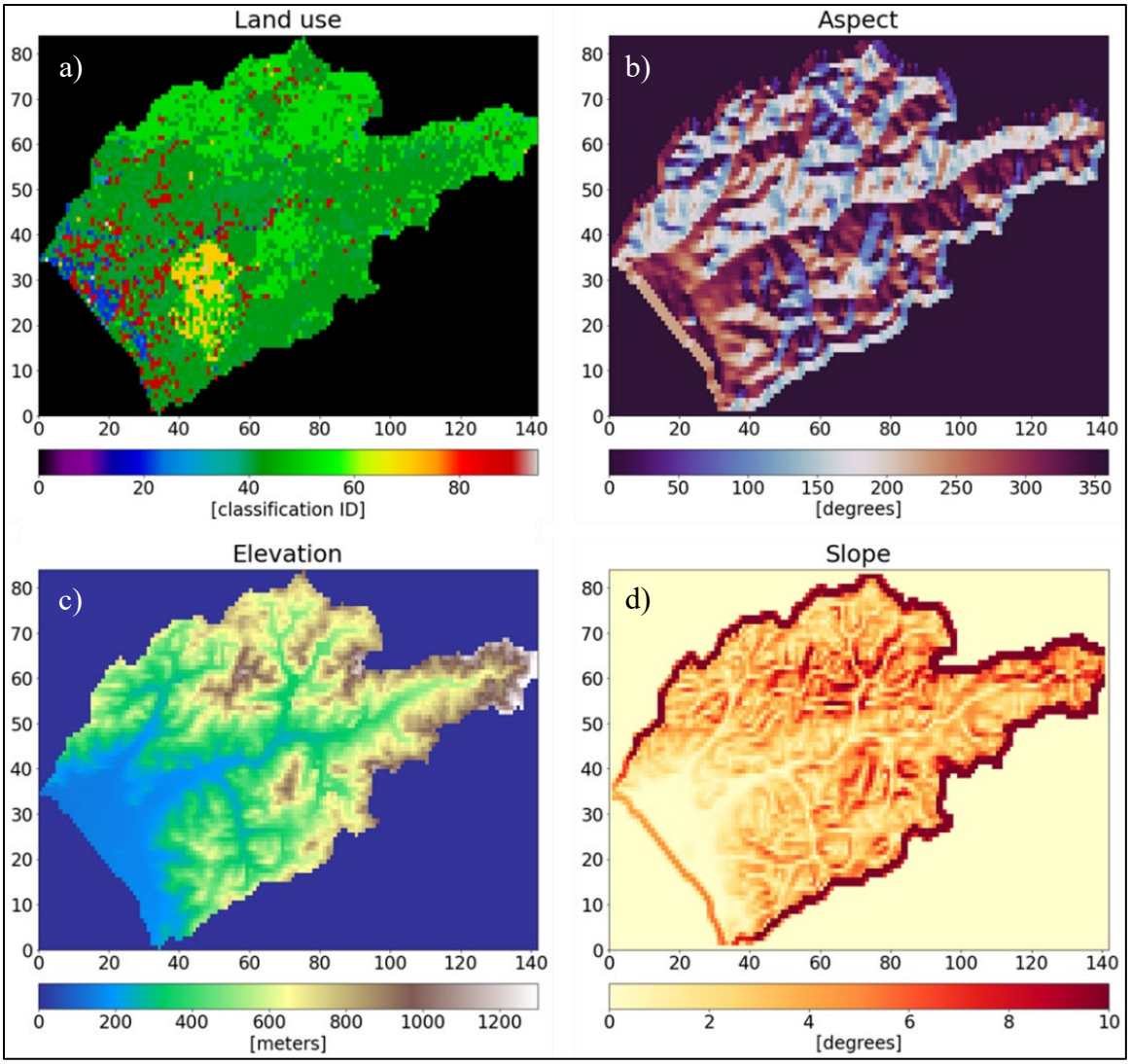

Figure 3. Landscape characteristics within the Chena River watershed with land use (*a*), aspect (*b*), elevation (*c*), and slope (*d*).

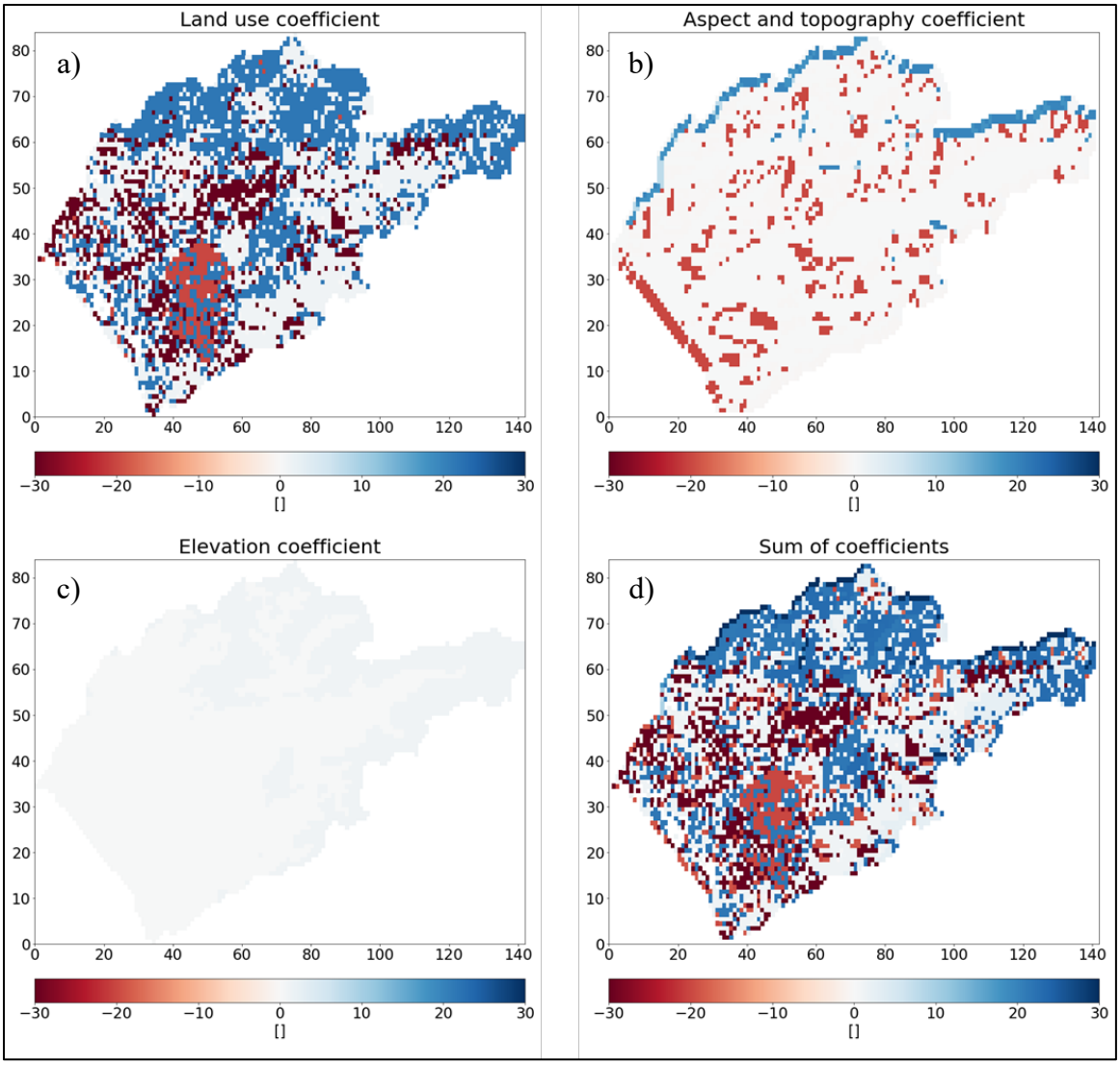

Figure 4. Chena River watershed coefficients for land use (*a*), aspect and topography (*b*), elevation (*c*), and sum of *a*, *b*, and *c* (*d*) (i.e., *Z* in Equation 1).

RESULTS: We derived the probability of near-surface permafrost (Figure 5*a*) by using the sum of coefficients in Figure 4 (*Z*) within Equation 1. Using this method, the majority of the domain (71.9%) has a high probability of permafrost (shades of *blue*). However, some areas in the central and western portions of the domain have a low probability of permafrost (shades of *red*). This seems to be largely due to negative land use coefficients in these areas, e.g., grassland/herbaceous in the south-central area and a stretch of deciduous forest in the central area.

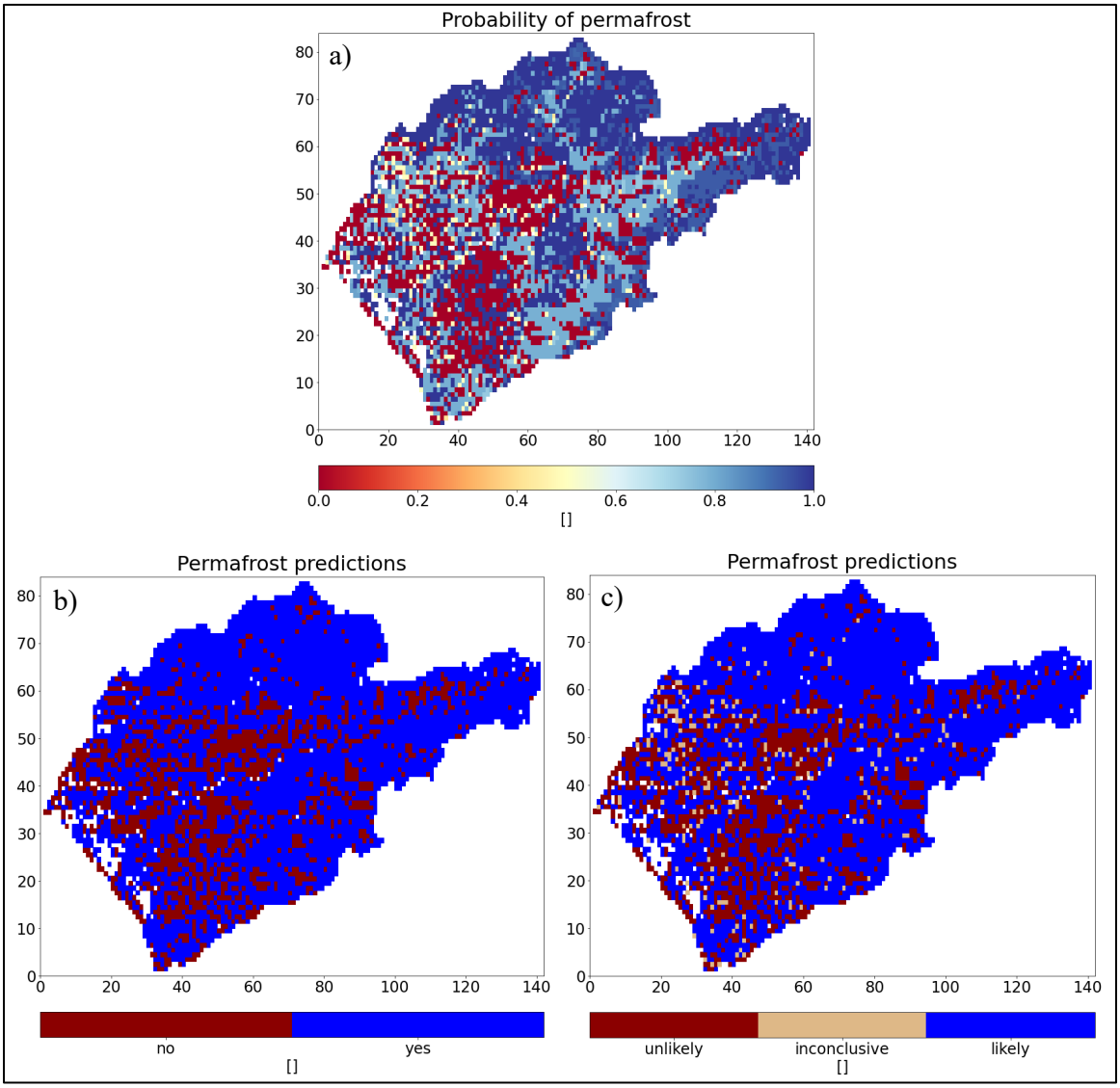

Figure 5. Probability of near-surface permafrost for the Chena River watershed using the sum of coefficients method (higher values indicate higher probability of permafrost) (*a*). Categorical near-surface permafrost predictions using coefficient thresholds as defined by Panda et al. (2010) (*yes* = permafrost; *no* = no permafrost) (*b*), and a textual category method similar to that described by the IPCC (Mastrandrea et al. 2010; Arias et al. 2023) (*c*).

Figures 5*b* and 5*c* show categorical representations of the permafrost probabilities in Figure 5*a*. Figure 5*b* uses the thresholds defined in Panda et al. (2010), i.e., "yes" for probabilities ≥0.5 and "no" for probabilities <0.5. On the other hand, Figure 5*c* uses a three-category method similar to that employed in the recent IPCC reports, equating a textual "category" with the likelihood of a particular quantitative outcome (Mastrandrea et al. 2010; Arias et al. 2023). This method includes a binary "likely-unlikely" system for predicting permafrost occurrence as well as a middle category—inconclusive—for which grid cells have a probability between 0.333333 and 0.666666. Using this method does not yield many inconclusive results (Figure 5*c*). Of the 5,598 nonnull values, only 219 of them (3.9%) fall into the "inconclusive" category. This means that the vast majority of grid cells in the Chena River watershed are either "likely" or "unlikely" to include permafrost when using this system.

SUMMARY: This technical note presents preliminary results for predicting near-surface permafrost in the Chena River watershed in central Alaska using a methodology initially developed by Panda et al. (2010). Our results show that land use is the dominant factor in predicting near-surface permafrost within our study region. This is likely due to the high absolute values for the land use coefficient throughout most of the region. Other variables, such as aspect/topography and elevation, had a more minor role in these predictions. Shifting to a three-category methodology similar to that used in recent IPCC reports produced very few "inconclusive" values; the vast majority of grid cells fell into either the "likely" or "unlikely" prediction categories for permafrost existence.

Vuyovich and Daly (2012) also produced a permafrost map of the Chena River watershed using a methodology nearly identical to the one used in this work (based on that of Panda et al. 2010). However, direct comparisons between their map and ours are difficult for two reasons, (1) the southern portion of the Chena River watershed that we analyzed in this work is absent from the map produced by Vuyovich and Daly (2012) and (2) their map has a much higher spatial resolution than ours (60-m resolution for their digital elevation model). That said, a first-order comparison between our map and theirs reveals some similarities and differences. Both maps have more frequent "no permafrost" values along the main Chena River channel and in the western portion of the watershed, yet their map has a much greater density of "no permafrost" values in the western portion of the watershed.

Our results can be improved through refinement of the algorithm and method presented herein. Perhaps the most important recommendation and improvement is to pursue a validation of these permafrost predictions using field measurements. Another improvement would be to filter out the spurious edge effect in the aspect and slope data (Figures 3 and 4). Additional improvements could include creating coefficients for latitude and revising the coefficients for elevation, since it is possible that permafrost could form in certain high-latitude or high-altitude locations regardless of land use and aspect. Assuming that these improvements are successful, this methodology could ultimately be extended to other cold regions where discontinuous permafrost is known to be present.

ADDITIONAL INFORMATION: The Open Researcher and Contributor ID (ORCiD) numbers for the authors are the following: Dr. Ross E. Alter 0000-0003-3730-4641; Dr. Nawa Raj Pradhan 0000-0001-5210-0896, and Dr. Anna M. Wagner 0000-0002-8678-1279.

This technical note is funded by the US Army Military Engineering Program through work item number 12JCJ0 and should be cited as follows:

> Alter, R. E., N. R. Pradhan, and A. M. Wagner. 2023. *Preliminary Permafrost Predictions within the Chena River Watershed, Alaska, Using Landscape Characteristics*. ERDC TN-24-2. Vicksburg, MS: Engineer Research and Development Center. http://dx.doi.org/10.21079/11681/48074.

REFERENCES

Arias, P. A., N. Bellouin, E. Coppola, R. G. Jones, G. Krinner, J. Marotzke, V. Naik, et al. 2023. "Technical Summary," In *Climate Change 2021–The Physical Science Basis*, eds. V. Masson-Delmotte, P. Zhai, A. Pirani, S. L. Connors, C. Péan, S. Berger, N. Caud, et al. Cambridge: Cambridge University Press, 33−144. https://doi.org/10.1017/9781009157896.

Homer, C., and J. Dewitz. 2019. "NLCD 2016." [Data set]. *NLCD (National Land Cover Database)*. Sioux Falls, SD: USGS–Earth Resources Observation and Science (EROS) Center. https://www.usgs.gov/data/nlcd-2016.

Jorgenson, M., K. Yoshikawa, M. Kanevskiy, Y. Shur, V. Romanovsky, S. Marchenko, G. Grosse, J. Brown, and B. Jones. 2008. "Permafrost Characteristics of Alaska." *Proceedings of the Ninth International Conference on Permafrost*. https://www.researchgate.net/publication/269040421_Permafrost_characteristics_of_Alaska.

Mastrandrea, M. D., C. B. Field, T. F. Stocker, O. Edenhofer, K. L. Ebi, D. J. Frame, H. Held, et al. 2010. "Guidance Note for Lead Authors of the IPCC Fifth Assessment Report on Consistent Treatment of Uncertainties." *Intergovernmental Panel on Climate Change (IPCC)*. https://www.ipcc.ch/site/assets/uploads/2018/05/uncertainty-guidance-note.pdf

Panda, S. K., A. Prakash, D. N. Solie, V. E. Romanovsky, and M. T. Jorgenson. 2010. "Remote sensing and field-based mapping of permafrost distribution along the Alaska Highway corridor, interior Alaska." *Permafrost and Periglacial Processes* 21(3): 271-281. https://doi.org/https://doi.org/10.1002/ppp.686.

Pradhan, N. R., C. W. Downer, and S. Marchenko. 2019. "Catchment Hydrological Modeling with Soil Thermal Dynamics During Seasonal Freeze-Thaw Cycles." *Water* 11 (1): 116. http://dx.doi.org/10.3390/w11010116.

Pradhan, N. R., C. W. Downer, S. Marchenko, A. Lijedahl, T. A. Douglas, and A. Byrd. 2013. *Development of a Coupled Framework for Simulating Interactive Effects of Frozen Soil Hydrological Dynamics in Permafrost Regions*. ERDC TR-13-15. Vicksburg, MS: Engineer Research and Development Center. https://hdl.handle.net/11681/8474.

USGS. 2023. *1 Arc-second Digital Elevation Models (DEMs) - USGS National Map 3DEP Downloadable Data.* USGS. https://www.sciencebase.gov/catalog/item/4f70aa71e4b058caae3f8de1

Vuyovich, C. M., and S. F. Daly. 2012. *The Chena River Watershed Hydrology Model*. ERDC/CRREL TR-12-1. Hanover, NH: Engineer Research and Development Center–Cold Regions Research and Engineering Laboratory. https://hdl.handle.net/11681/5364.